Macromolecules

pubs.acs.org/Macromolecules
Article

Design of Linear Block Copolymers and *ABC* Star Terpolymers That Produce Two Length Scales at Phase Separation

Merin Joseph,* Daniel J. Read,* and Alastair M. Rucklidge*

Cite This: *Macromolecules* 2023, 56, 7847−7859
Read Online

ACCESS | Metrics & More | Article Recommendations

ABSTRACT: Quasicrystals (materials with long-range order but without the usual spatial periodicity of crystals) were discovered in several soft matter systems in the last 20 years. The stability of quasicrystals has been attributed to the presence of two prominent length scales in a specific ratio, which is 1.93 for the 12-fold quasicrystals most commonly found in soft matter. We propose design criteria for block copolymers such that quasicrystal-friendly length scales emerge at the point of phase separation from a melt, basing our calculations on the Random Phase Approximation. We consider two block copolymer families: linear chains containing two different monomer types in blocks of different lengths, and *ABC* star terpolymers. In all examples, we are able to identify parameter windows with the two length scales having a ratio of 1.93. The models that we consider that are simplest for polymer synthesis are, first, a monodisperse A_LBA_SB melt and, second, a model based on random reactions from a mixture of A_L, A_S, and *B* chains: both feature the length scale ratio of 1.93 and should be relatively easy to synthesize.

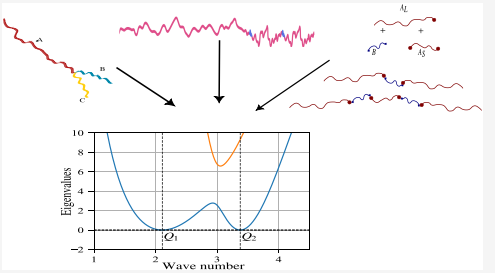

INTRODUCTION

Quasicrystals are crystals that have long-range order, and so have sharp X-ray diffraction spectra, and yet do not have the spatial periodicity usually associated with crystals.[1] They often have rotation symmetries that are incompatible with spatial periodicity. The first examples were in metal alloys and had icosahedral symmetry.[2] Subsequently, Zeng et al.[3] reported quasicrystals in micelles made from wedge-shaped dendrimers: these examples were quasicrystalline, with 12-fold rotation symmetry in two dimensions and periodic in the third. 12-Fold quasicrystals have recently been reported in systems as simple as oil−water−surfactant mixtures.[4] An earlier discovery by Hayashida et al.[5] was an example with the same dodecagonal rotation symmetry in a three-component *ABC* star terpolymer blend of polyisoprene, polystyrene, and poly(2-vinylpyridine). In this case, the bulk properties were as if the three components were immiscible, forming tiles composed of the *A*, *B*, and *C* block copolymers in two dimensions, with the junction points aligned in the third. The small-angle X-ray scattering pattern of the quasicrystal sample had two circles of wavevectors with 12 peaks on each circle, demonstrating dodecagonal rotation symmetry and the presence of two length scales, roughly in a ratio of 1:1.93.

Block copolymers offer versatility in the structures they can form owing to the wide variety of different monomers, the different ways that the monomers can interact, and the control of the lengths of the monomer chains.[6] Several recent papers use this versatility to choose polymers in such a way as to form quasicrystal approximants, for example, by choosing different monomer types in diblock micelles,[7,8] in giant surfactants,[9] in polymer liquid crystal systems,[10] and in *ABC* triblock copolymers.[11] The potential diversity of resultant mesoscale structures in block copolymer systems is explained in detail in the review by Huang et al.[12] These structures offer the potential of developing materials with unusual photonic bandgap behavior.[13,14]

There is experimental evidence that quasicrystals are associated with the presence of two length scales in the system[5,12] in a wide range of examples going beyond soft matter and materials science (for example, fluid dynamics[15−17] and nonlinear optics[18]). The presence of different length scales is qualitatively clear in the structure of the components for several of the soft matter systems that form QCs, including micelles with a soft corona[3,19] and star copolymers with arms of different lengths.[5,20] The connection between having two length scales and the stability of QCs is supported by a large body of theoretical work, including from the fields of fluid dynamics and pattern formation,[1,15,21−26] phase field crystals,[27−34] classical density functional theory of interacting particles,[35−41] molecular dynamics,[42,43] and self-assembly of hard particles[44,45] and hard particles with shoulder potentials.[46,47] At the most basic level, the theoretical work attributes the stability of QCs to the nonlinear three-wave interaction of waves of density fluctuations

Received: April 25, 2023
Revised: September 4, 2023
Published: September 26, 2023

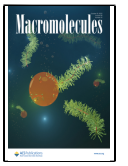

https://doi.org/10.1021/acs.macromol.3c00800
Macromolecules 2023, 56, 7847−7859

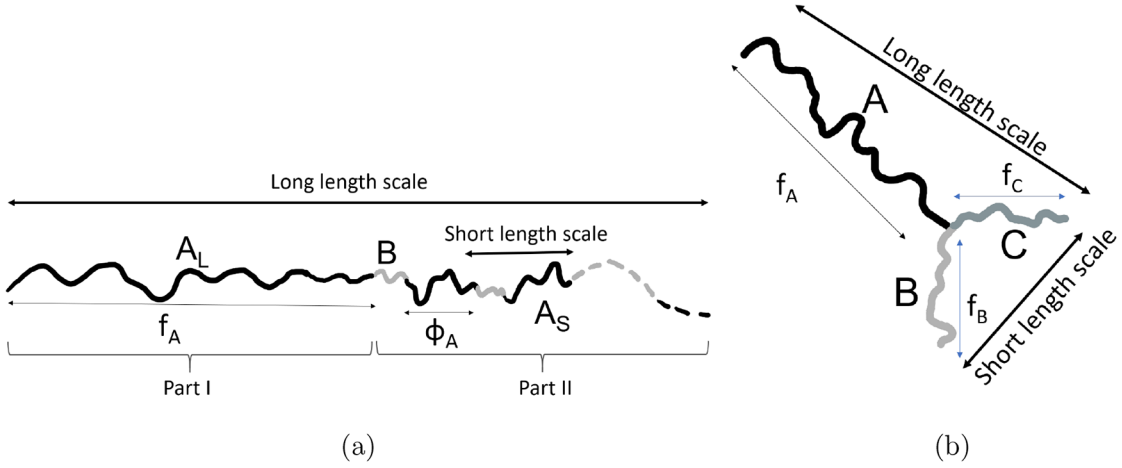

Figure 1. Schematic models for the block copolymers. (a) $A_L(BA_S)_n$ with A in black and B in gray, and L and S indicating the long and short A blocks. The length fraction (of the total polymer length) of the long A block in part I is f_A, and within part II, ϕ_A is the length fraction of the short A blocks within each of the n BA_S diblocks. (b) ABC star block copolymer with A in black, B in light gray, and C in midgray, having length fractions f_A, f_B, and f_C, respectively.

on the two length scales. For example, when the ratio of those length scales is $2\cos 15° \approx 1.93$, the nonlinear interactions between two waves of one length scale and one of the other favor density waves that are spaced 30° apart in Fourier space,[15−17,25,48,49] giving 12-fold symmetry. These arguments suggest that the length scales should usually be within a factor of 2 of each other to encourage QCs, with a ratio of 1.93 for 12-fold QCs and 1.618 for 10-fold or icosahedral QCs,[1,22,24,29,49,50] with other ratios stabilizing other quasicrystals.[51] Nevertheless, stable QCs can also be found with larger ratios, for example, an 8-fold quasipattern was found in a reaction−diffusion problem with a length scale ratio of 4.[26]

The theoretical arguments attribute the stability of QCs to the presence of two length scales, but this presence is not sufficient for the formation of QCs: even with two length scales, hexagons, lamellae or other structures of different sizes can be stable. Nor is the presence of two length scales necessary for the formation of QCs: in fluid dynamics, there are examples of quasipatterns in Faraday wave experiments[52] whose stability can be explained in the context of a single length scale.[21,49] Nonetheless, the presence of two length scales in an appropriate ratio is strongly associated with the stability of QCs,[31] though some tuning of parameters is usually needed to ensure that QCs are favored over competing crystalline phases such as hexagons and lamellae.[38]

In this paper, we focus on what features in the polymer design can lead to two length scales in the instability toward phase separation. We will work in the weak segregation limit and use the random phase approximation (RPA) to characterize the length scales that emerge, concentrating on the point of phase separation of block copolymer melts. This complements other theoretical approaches to this problem, for example, using self-consistent field theory.[53−55] The advantage of using the simpler RPA theory is that it allows a rapid search through parameter space for likely candidates of two length scale phase separation. The disadvantage is that the theory does not predict which structure will ultimately be stable.

Prior work in this area[56−58] considered a limited range of architectures giving rise to two length scales. Here, we extend their work by (i) working within the same classes of architecture but increasing the explored parameter space, (ii) extending the investigation to include copolymers formed by random reaction, and (iii) considering three-component star polymers of the form investigated by Hayashida et al.[5] One focus, especially within themes (i) and (ii) above, has been to find structures that are as simple as possible to synthesize while retaining the two length scale feature.

We consider two classes of polymer architectures, both chosen to allow two length scales to emerge, see Figure 1, and ask whether there is one or two length scales, and in the latter case, how can the ratio of these length scales be controlled? The first class has two types of monomers (A and B), while the second has three (A, B, and C). Each example is specified by the proportions of the different components and the strengths of the interactions between them. The selection of length scales during phase separation involves a balance between the entropy of stretching the polymer chain and the energy penalty of having incompatible monomers interacting. Qualitatively, the phase separation length scales are set by the size of subsections of the chain that repel one another. To achieve phase separation simultaneously at two length scales requires fine-tuning of the relative degrees of repulsion via composition and interaction parameters. Typically, one requires greater average repulsion (per monomer) to drive phase separation at the short length scale because the stretching energy is larger; conversely, less repulsion is needed at the longer length scale. These qualitative features are present in all examples explored below.

Linear block copolymers are much easier to manufacture compared to branched block copolymers, so our first class of polymer (Figure 1a) explores the design of linear block copolymers. Block copolymers that are manufactured will normally exhibit polydispersity, but we start with a discussion of idealized monodisperse models before introducing some aspects of polydispersity via random assembly of the blocks. A similar architecture was considered by Nap,[56] but they restricted their investigation to cases where the A_S and B blocks are of equal length; here we show that relaxing that constraint leads to greater flexibility in the design space and the possibility of easier synthesis. The monodisperse chains have a long section A_L of A-type monomers followed by n alternating BA_S diblocks, with shorter stretches of B-type and A-type monomers linked back to back. Microphase separation of the long A_L block and the $(BA_S)_n$ tail gives one length scale, while the incompatibility between A

https://doi.org/10.1021/acs.macromol.3c00800
Macromolecules 2023, 56, 7847−7859

and B sub-blocks within the tail can lead to microphase separation on a second length scale. The presence of A monomers in the BA_S tail reduces the incompatibility between it and the A_L section. Polydispersity is achieved by starting with a mixture of A_L, A_S, and B blocks. These are allowed to react in such a way that each B block links to an A block at either end, the A_S blocks link to B blocks at either end, while the A_L blocks only react with B blocks at one end. The result is a mixture of polymers of different lengths, starting and ending with A_L blocks but with different lengths of $BA_S\cdots A_SB$ blocks in between, consistent with the proportions in the initial mixture.

The second class of polymers (Figure 1b) is an ABC star structure, with different lengths of the A, B and C arms, inspired by the polymers used by Hayashida et al.[5] Here, two length scales can emerge if one arm (A) is longer than the other two (B and C), with microphase separation between A and B with C together leading to the long length scale, and microphase separation between B and C leading to the short length scale. Again, this class has been explored in the literature;[59] the new perspective here is the focus on phase separation with two length scales.

In each case, we explore the parameter ranges in which two length scales emerge, and we indicate the parameters for which the ratio between the two length scales would favor 12-fold quasicrystals. This work is part of a long-term effort to develop design criteria for polymers that will robustly and spontaneously form quasicrystals.

Our main tool is the random phase approximation (RPA) for polymer blends, which is the truncation of the free energy functional at the quadratic term in density fluctuations.[60,61] The theory describes the point at which there is a transition from a polymer melt to a phase-separated structure, near the point of the initial segregation. As a result, the theory does not identify the final stable phase. The method uses coarse-graining of monomers into monomer units with effective bond length (or Kuhn length) b, which allows the polymer to be considered as consisting of flexible and freely rotating units that can be described as a random walk. Microphase separation occurs when there are density fluctuations that decrease the free energy of the homogeneous melt, and the wavenumber of these fluctuations gives the preferred length scale of the resulting phase-separated structure. The melt phase is (meta-)stable when a (small) density fluctuation of any wavenumber increases the free energy.

In the case of an incompressible melt with two monomer types A and B, and in the absence of any specific interaction between the monomer types other than incompressibility interactions, the RPA is concerned with the noninteracting structure factor $S_0(q)$ of the homogeneous and isotropic melt. This noninteracting incompressible structure factor depends on wavenumber q and is expressed in terms of correlations between small random composition fluctuations, as described in more detail below.

Interactions between the monomer units are parametrized by the Flory interaction parameter χ_{AB}, which is related to the interaction energies between the different monomer types. Including these interactions leads to additional composition correlations that are described in terms of the structure factor $S(q)$. This structure factor also gives the form of the expected results of scattering in experiments that detect composition fluctuations in the melt.

In an incompressible two-component (A and B) copolymer, consisting of lengths of A units joined to lengths of B units, possibly with repetition or branching, and with a Flory interaction parameter χ_{AB}, the structure factor S is related to the noninteracting structure factor S_0 by[62]

$$S(q) = \left(\frac{1}{S_0(q)} - \frac{2\chi_{AB}}{\Omega\rho}\right)^{-1} \tag{1}$$

where Ω is the system volume and ρ is the monomer unit density, so $\Omega\rho$ is the total number of monomer units. When there are no interactions ($\chi_{AB} = 0$), the two structure factors are the same. The noninteracting structure factor $S_0(q)$ is positive and may have a maximum at a particular wavenumber, so $S_0(q)^{-1}$ may have a positive minimum. As interactions are introduced (as χ_{AB} increases), $S(q)$ goes to infinity at the value of χ_{AB} for which the term in brackets in eq 1 first goes to zero, and so phase separation occurs on the length scale corresponding to the wavenumber at which $S_0(q)$ is maximum. If $S_0(q)$ has two maxima of equal height at different wavenumbers, eq 1 indicates that phase separation will happen simultaneously at both wavenumbers.

There are more general expressions for compressible systems and for copolymers with more than two types of monomer. In these cases, the RPA is formulated by writing the free energy as a quadratic functional of the composition fluctuations, with multiple Flory interaction parameters. For the melt to be stable, this quadratic form needs to be positive definite, so phase separation occurs when eigenvalues of the quadratic form change sign.

Read[63] formulated a method to find the noninteracting structure factor for an arbitrary block copolymer melt, using "self-terms", "coterms" and "propagator terms" to describe the architecture of the block copolymer, tracing the arrangement and connections between blocks in the chain. Here, the self-terms describe the density correlations between monomer units within a single block, and the coterms describe the density correlations between monomer units from two different blocks on the same polymer. The chain between two different blocks may have other blocks in between, depending on the architecture of the polymer, and the propagator terms specify how the correlations (given by coterms) are modified by the presence of the intermediate blocks. We use this method to compute the structure factor for our two classes of copolymer architecture.

TWO-COMPONENT LINEAR CHAIN WITH FIXED ARCHITECTURE

In our two-component block copolymer system shown in Figure 1(a), we index each polymer chain within the system by α, so $1 \le \alpha \le n_c$, where n_c is the number of chains. Within each chain α, we index the location of each monomer unit by l, with $1 \le l \le N$, where N is the number of monomer units in each chain, assumed (in this section) to be the same for each chain. The location of the monomer unit is thus $\boldsymbol{r}_l^\alpha$, and each monomer unit is of type A or type B. The density of A monomer units in physical space is then a sum of delta functions, summed over all chains and all locations on each chain of the A monomer units, and similarly for B. The Fourier transforms of these two density distributions are then

$$\rho_{\boldsymbol{q}}^A = \sum_A \exp(i\boldsymbol{q}\cdot\boldsymbol{r}_l^\alpha)$$
$$\rho_{\boldsymbol{q}}^B = \sum_B \exp(i\boldsymbol{q}\cdot\boldsymbol{r}_l^\alpha) \tag{2}$$

https://doi.org/10.1021/acs.macromol.3c00800
Macromolecules 2023, 56, 7847−7859

where $\boldsymbol{q}$ is the wavevector, and the sums are taken over the locations of the A and B monomer units. The structure factors for the A and B monomer units in the absence of any interactions are given by the correlations in the densities of the two types, which in Fourier space can be written as

$$S_0^{AA}(q) = \langle \rho_{-\boldsymbol{q}}^A \rho_{\boldsymbol{q}}^A \rangle_0$$
$$S_0^{AB}(q) = \langle \rho_{-\boldsymbol{q}}^A \rho_{\boldsymbol{q}}^B \rangle_0 = S_0^{BA}(q)$$
$$S_0^{BB}(q) = \langle \rho_{-\boldsymbol{q}}^B \rho_{\boldsymbol{q}}^B \rangle_0 \tag{3}$$

where the angle brackets with subscript 0 represent the average over all possible configurations of the polymers in the absence of any interactions between monomers, within the constraints of the polymer architecture.

The incompressibility constraint requires $\rho_{\boldsymbol{q}}^A = -\rho_{\boldsymbol{q}}^B = \rho_{\boldsymbol{q}}$, so we need only use $\rho_{\boldsymbol{q}}$ in place of $\rho_{\boldsymbol{q}}^A$ and $-\rho_{\boldsymbol{q}}$ in place of $\rho_{\boldsymbol{q}}^B$. Using the RPA,[61] we can express the incompressible structure factor in the absence of interactions as

$$S_0(q) = \frac{S_0^{AA} S_0^{BB} - (S_0^{AB})^2}{S_0^{AA} + S_0^{BB} + 2S_0^{AB}} \tag{4}$$

and the free energy functional up to second order in density fluctuations (in units of $k_B T$) as

$$F\{\rho_{\boldsymbol{q}}\} = \frac{1}{2} \sum_{\boldsymbol{q}} \rho_{\boldsymbol{q}} \rho_{-\boldsymbol{q}} \left(\frac{1}{S_0(q)} - \frac{2\chi_{AB}}{\Omega\rho} \right) \tag{5}$$

If the term in brackets in eq 5 is positive for all wavenumbers, the melt is (meta-)stable, while if this term changes sign, the melt is unstable. So, as in the discussion of eq 1, the length scale of phase separation is associated with a maximum of $S_0(q)$.

In eq 5, $\Omega\rho$ is equal to the total number of monomer units, and with n_c chains each having N monomer units, we have $\Omega\rho = n_c N$. We see below that $S_0(q)$ is proportional to $n_c N^2$, so by treating the Flory interaction parameter χ_{AB} in combination with N, all dependence on N can be isolated into $N\chi_{AB}$.

We use the method of Read[63] to calculate the terms $S_0^{AA}(q)$, $S_0^{AB}(q)$, and $S_0^{BB}(q)$ in the absence of any interaction between the monomers, for the $A_L(BA_S)_n$ structure, previously considered by Nap,[56] and shown in Figure 1(a). The method treats each polymer chain α by splitting it into different blocks, with each block being of a single monomer type. We illustrate this in Figure 2, with γ and γ' indicating two different blocks. Each block is associated with a "self-term" J_γ, a "coterm" H_γ and a "propagator term" G_γ.[63] The self-term for an individual block γ gives the contribution to the structure factor from that block, and comes from summing over monomer pairs within that block. The contribution from the interaction between two blocks γ and γ' is the coterm for block γ multiplied by the propagator terms of all of the blocks on the unique connecting path between γ and γ' (see Figure 2), and finally multiplied by the coterm for block γ' at the end. This contains all pairwise monomer interactions between monomers in the two blocks γ and γ'. The structure factor for a given polymer chain α is then a combination of the sum of the self-terms for each block and a double sum of the product of coterms with appropriate propagators over all nonidentical pairs of blocks in that chain.

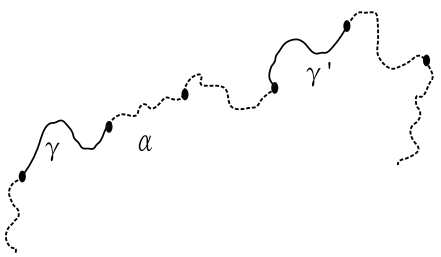

Figure 2. We index each polymer chain within the system by α, and γ and γ' are two blocks within the chain (these could be A_L, A_S, or B).

Each block γ has its own normalized wavenumber Q_γ, dependent on the number of monomer units N_γ in the block

$$Q_\gamma^2 = \frac{N_\gamma b^2}{6} q^2 \tag{6}$$

where $q = |\boldsymbol{q}|$. This wavenumber is scaled by the effective bond length b; for the sake of simplicity, we take the same length b for all blocks. Each of the self-, co-, and propagator terms are functions of these normalized wavenumbers Q_γ for each block γ. These terms are all based on Debye functions[60] and are given by[63]

$$\text{self-term: } J_\gamma = N_\gamma^2 j\left(Q_\gamma^2\right) \quad \text{where } j(Q^2) = \frac{2}{Q^4}(\exp(-Q^2) - 1 + Q^2)$$
$$\text{coterm: } H_\gamma = N_\gamma h\left(Q_\gamma^2\right) \quad \text{where } h(Q^2) = \frac{1}{Q^2}(1 - \exp(-Q^2))$$
$$\text{propagator term: } G_\gamma = \exp\left(-Q_\gamma^2\right) \tag{7}$$

Turning now to the specific $A_L(BA_S)_n$ architecture, the polymer chain is considered in two parts. Part I is the A_L block with length fraction f_A, and part II is the tail $(BA_S)_n$, comprising n BA_S diblocks, with length fraction $1 - f_A$. Within each BA_S diblock, the A_S block has a length fraction of ϕ_A and hence length fraction of the B block is $1 - \phi_A$. If the total number of monomer units in a chain is N, then the number of A and B units in each block of the polymer chain can be written down

number of A monomer units in the A_L block in part I:

$$N_{A_L} = f_A N$$

number of A monomer units in each A_S block in part II:

$$N_{A_S} = \frac{1}{n}(1 - f_A)\phi_A N$$

number of B monomer units in each B block in part II:

$$N_B = \frac{1}{n}(1 - f_A)(1 - \phi_A) N \tag{8}$$

We note that the two types of A chain have the same lengths when $N_{A_L} = N_{A_S}$, or

$$\phi_A = n \frac{f_A}{1 - f_A} \tag{9}$$

For the specific $A_L(BA_S)_n$ polymer, the three normalized wavenumbers Q_{A_L}, Q_{A_S}, and Q_B are given by

$$Q_{A_L}^2 = f_A Q^2$$
$$Q_{A_S}^2 = \frac{1}{n}(1 - f_A)\phi_A Q^2$$
$$Q_B^2 = \frac{1}{n}(1 - f_A)(1 - \phi_A) Q^2 \tag{10}$$

https://doi.org/10.1021/acs.macromol.3c00800
Macromolecules 2023, 56, 7847−7859

where $Q^2 = \frac{Nb^2}{6}q^2$.

To calculate the structure factor, we start by treating parts I and II separately, and we illustrate the calculation for the case $n = 2$ before discussing the case of general n.

In part I, there is only the A_LA_L self-term

$$J^I_{AA} = J_{A_L} = N^2_{A_L} j(Q^2_{A_L}) = N^2 f^2_A j(f_A Q^2) \tag{11}$$

There are no J^I_{BB} and J^I_{AB} self-terms. We have given the explicit dependence on N_{A_L} and Q_{A_L}, and on N and Q, in this case, but we will suppress this below. We note that, here and below, all terms and the final expressions can written as functions of the scaled wavenumber Q, and that the self-terms, and the coterm−propagator term−coterm combinations, will be proportional to N^2.

In part II, we work out composite self-terms for the $(BA_S)_2 = BA_SBA_S$ chain: J^{II}_{AA}, J^{II}_{BB}, and J^{II}_{AB}. For J^{II}_{AA}, each A_S block can interact with itself, yielding a self-term J_{A_S} multiplied by 2 since there are two of these. Each A_S block can also interact with the other A_S block: for this A_SA_S interaction, we use a coterm (H_{A_S} at each end) and a propagator term (G_B) to jump across the B block. There is a factor of 2 since the interaction since either A_S block could be the starting point. Putting these together results in

$$J^{II}_{AA} = 2J_{A_S} + 2H_{A_S}G_BH_{A_S} \tag{12}$$

Similarly, J^{II}_{BB} is calculated by considering the two self-terms J_B and the coterm−propagator term−coterm chain in each direction

$$J^{II}_{BB} = 2J_B + 2H_BG_{A_S}H_B \tag{13}$$

The last term within part II is J^{II}_{AB}, starting with an A_S block and ending with a B block. In this case, we have coterms $H_{A_S}H_B$ for every instance of adjacent A_S and B blocks, and we have coterm−propagator term−propagator term−coterm chains for the A_S and B blocks separated by the other A_S and B blocks

$$J^{II}_{AB} = 3H_{A_S}H_B + H_BG_{A_S}G_BH_{A_S} \tag{14}$$

There is an equal expression for J^{II}_{BA}, starting with a B block and ending with an A_S block.

Finally, we consider interactions between parts I and II. The A_L block has the self-term J_{A_L} and coterm H_{A_L}, and will interact with the A_S blocks and B blocks in part II. The AA interactions lead to contributions $2H_{A_L}G_BH_{A_S}$ and $2H_{A_L}G_BG_{A_S}G_BH_{A_S}$, with the factor 2 in each case since the AA interactions can start with A_L or A_S. The AB interactions, starting with A_L and ending with B, are $H_{A_L}H_B$ and $H_{A_L}G_BG_{A_S}H_B$.

These contributions are combined to give the three terms

$$\begin{aligned} S_0^{AA} &= n_c(J^I_{AA} + J^{II}_{AA} + 2H_{A_L}G_BH_{A_S} + 2H_{A_L}G_BG_{A_S}G_BH_{A_S}) \\ S_0^{AB} &= n_c(J^{II}_{AB} + H_{A_L}H_B + H_{A_L}G_BG_{A_S}H_B) \\ S_0^{BB} &= n_c\, J^{II}_{BB} \end{aligned} \tag{15}$$

where we have multiplied by the number of chains n_c.

In the case of general n, the part I term remains the same. For the other terms, we end up with longer expressions involving additional powers of $G_{A_S}G_B$ propagator terms. After some combinatorics, and summing the resulting finite geometric series, the general n composite self-terms for part II are

$$\begin{aligned} J^{II}_{AA} &= nJ_{A_S} + 2H^2_{A_S}G_B\left(\frac{n(1 - G_{A_S}G_B) - (1 - (G_{A_S}G_B)^n)}{(1 - G_{A_S}G_B)^2}\right) \\ J^{II}_{BB} &= nJ_B + 2H^2_BG_{A_S}\left(\frac{n(1 - G_{A_S}G_B) - (1 - (G_{A_S}G_B)^n)}{(1 - G_{A_S}G_B)^2}\right) \\ J^{II}_{AB} &= H_{A_S}H_B\left(\frac{(2n + 1)(1 - G_{A_S}G_B) - 2 + (G_{A_S}G_B)^n + (G_{A_S}G_B)^{n+1}}{(1 - G_{A_S}G_B)^2}\right) \end{aligned} \tag{16}$$

There is an equal expression for $J^{II}_{BA} = J^{II}_{AB}$. Then, the three terms in the total structure factor, for n_c chains, are

$$\begin{aligned} S_0^{AA} &= n_c\left(J^I_{AA} + J^{II}_{AA} + 2H_{A_L}H_{A_S}G_B\left(\frac{1 - (G_{A_S}G_B)^n}{1 - G_{A_S}G_B}\right)\right) \\ S_0^{BB} &= n_c\, J^{II}_{BB} \\ S_0^{AB} &= n_c\left(J^{II}_{AB} + H^I_AH_B\left(\frac{1 - (G_{A_S}G_B)^n}{1 - G_{A_S}G_B}\right)\right) \end{aligned} \tag{17}$$

These three terms are proportional to n_cN^2 and are functions of the scaled wavenumber Q. The three terms are then combined to give the overall noninteracting incompressible structure factor $S_0(q)$ using eq 4, also proportional to n_cN^2 and a function of Q.

Typically, for phase separation on one length scale, the structure factor plot will have a single dominant peak. We have chosen the architecture $A_L(BA_S)_n$ in order to allow phase separation with two length scales, which will manifest as two maxima, at scaled wavenumbers Q_1 and Q_2 in the structure factor plot. An example of the resulting structure factor S_0 is plotted in Figure 3 with $f_A = 0.39225$, $\phi_A = 0.85$, and $n = 5$. In this example,

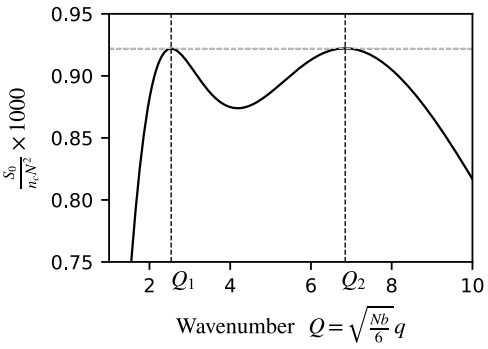

Figure 3. Incompressible structure factor S_0 (scaled by n_cN^2) from eq 4 as a function of scaled wavenumber Q for $f_A = 0.39225$, $\phi_A = 0.85$, and $n = 5$. The two maxima in the plot indicate the two length scales of phase separation. In this example, the wavenumbers at the maxima are $Q_1 = 2.53$ and $Q_2 = 6.85$, which have a ratio of 2.70, and the maxima are at the same height.

the structure factor has two maxima at the same height, and the wavenumbers at these two maxima are in the ratio 2.70. The two maxima will in general have different heights, with the higher one indicating the wavenumber that will appear first in phase separation. We define the ratio of wavenumbers $Q_r = Q_2/Q_1$, with $Q_1 < Q_2$.

https://doi.org/10.1021/acs.macromol.3c00800
Macromolecules 2023, 56, 7847−7859

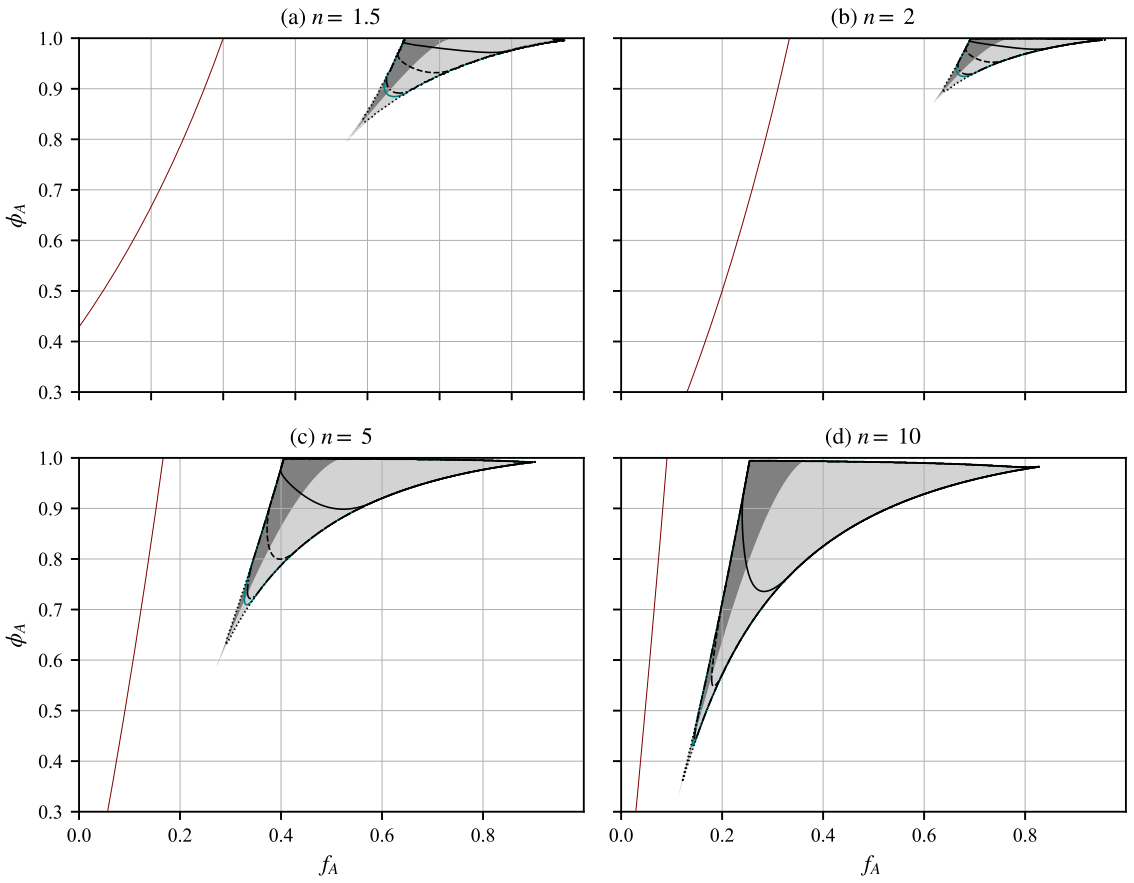

Figure 4. Regions of a single maximum (white) and two maxima (shaded), as a function of f_A and ϕ_A with $n = 1.5$, 2, 5, and 10. In the shaded regions, the darker (respectively, lighter) areas are where the maximum with the smaller (respectively, larger) wavenumber is higher. The solid contour line across the cusp indicates a wavenumber ratio $Q_r = 3.5$, with dashed, dash-dot, and dotted lines indicating wavenumber ratios of 2.5, 2.0, and 1.5, respectively. The teal line indicates parameter where the wavenumber ratio is 1.93. The maroon line is where the two types of A blocks have the same length, using eq 9.

Whether there is one maximum or two maxima, and their heights and values of the wavenumbers at the maxima, depends on the model parameters f_A, ϕ_A, and n. We have computed the structure factor for all possible combinations of f_A and ϕ_A, with $1 \leq n \leq 10$. A summary of the results is presented in Figure 4. As happens in other systems with transitions between one and two length scales, the boundary between the regions in parameter space separating one from two length scales are cusp-shaped.[56,58,64] Within the cusps (shaded), there are two maxima in the noninteracting structure factor and hence two length scales in the phase separation.

The architecture with $n = 1$, $A_L BA_S$, does not give any two length scale phase separation. The smallest model in the $A_L(BA_S)_n$ family that gives a cusp is that with $n = 2$ (Figure 4b), which is a linear chain with only 5 blocks. From Figure 4(b,c,d), we see that the area of the cusps increases with n, and the maximum ratio between the two length scales increases as well. This is because the short length scale is set by the size of the BA_S blocks, while the long length scale is set by the overall size of the polymer, which increases with n. The smallest linear chain with two components that gives two length scale phase separation is $A_L BA_S B$, indicated by $n = 1.5$ in Figure 4(a), with the structure factor computed along the same lines as described above.

We also show in Figure 4 the lines given by eq 9, where the two A blocks have the same lengths. We note that these lines do not intersect the cusps, which shows that having A blocks of different lengths is needed to have two length scales at the point of phase separation.

TWO-COMPONENT LINEAR CHAIN WITH RANDOM ASSEMBLY

The polydisperse model involves the random assembly of A_L, A_S, and B blocks using the Markov chain method proposed by Read.[63] In this model, the A_L blocks have one reactive end, the A_S blocks have two reactive ends, and the B blocks also have two reactive ends. The A reactive ends combine with B reactive ends to form linear chains. At the end of polycondensation, assuming a complete reaction and stoichiometry, the mixture will contain only chains that have A_L blocks at both ends and different lengths of $BA_S \cdots A_S B$ blocks in between, for example, $A_L BA_L$, $A_L BA_S BA_L$, etc., as illustrated in Figure 5.

The polycondensation process starts with initial block fractions β_{A_L}, β_{A_S}, and β_B for A_L, A_S, and B blocks, respectively, with $\beta_{A_L} + \beta_{A_S} + \beta_B = 1$. In the reaction, all of the B-type ends will react with A-type ends, so the initial mixture must contain the same number of each type. Thus

$$2n_{\text{blocks}}\beta_B = n_{\text{blocks}}\beta_{A_L} + 2n_{\text{blocks}}\beta_{A_S} \tag{18}$$

where n_{blocks} is the total number of blocks. Eliminating β_B, the condition for complete reaction is

$$3\beta_{A_L} + 4\beta_{A_S} = 2 \tag{19}$$

https://doi.org/10.1021/acs.macromol.3c00800
Macromolecules 2023, 56, 7847−7859

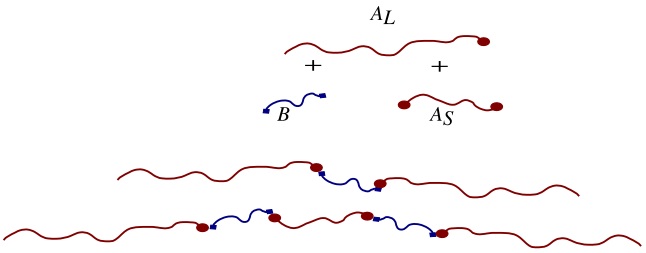

Figure 5. Schematic representation of the polydisperse model. Starting with a mixture of A_L, A_S, and B (top), the final mixture (bottom) will contain polymer chains of architecture A_LBA_L, $A_LBA_SBA_L$, etc.

In order to use the RPA for this system, we need the number of monomer units in each block. We use the number of monomer units in the A_L block (N_{A_L}) to scale the numbers in the A_S and B blocks (N_{A_S} and N_B), using scaling factors ν_{A_S} and ν_B

$$N_{A_S} = \nu_{A_S} N_{A_L}$$
$$N_B = \nu_B N_{A_L} \tag{20}$$

Thus, the three parameters that describe the model are β_{A_L}, ν_{A_S}, and ν_{A_S}.

Polymerization of such a mixture is by random assembly. At each stage in the polymerization, an A reactive end is always followed by a B block, while a B reactive end combines with A reactive ends from A_L or A_S blocks with probability given by the proportion of the two types. In terms of the model parameters, the probability that a B block will be followed by an A_L block is $P_{A_LB} = \frac{\beta_{A_L}}{2\beta_B}$ and that a B block will be followed by an A_S block is $P_{A_SB} = \frac{\beta_{A_S}}{\beta_B}$, so from eq 18, we have $P_{A_LB} + P_{A_SB} = 1$. The probabilities that a B block follows A_L or A_S blocks are both 1, and the probabilities of other combinations (for example, A_S followed by A_L) are zero.

This is a Markov process, where the block that gets attached depends only on the last block, and the structure factor can be computed by the methodology of Read.[63] The ideas are an extension of those discussed above, but with infinite rather than finite geometric series. For example, for the contribution to the S_0^{AA} part of the noninteracting structure factor from the A_L to A_L interactions, there are two coterm H_{A_L} factors for each end, as well as sums of propagator terms corresponding to all of the possible chains that can go between the two ends, weighted by the probability of that chain. So, a single B block contributes $P_{A_LB}G_B$, a BA_SB chain contributes $P_{A_SB}G_BG_{A_S}P_{A_LB}G_B$, a BA_SBA_SB

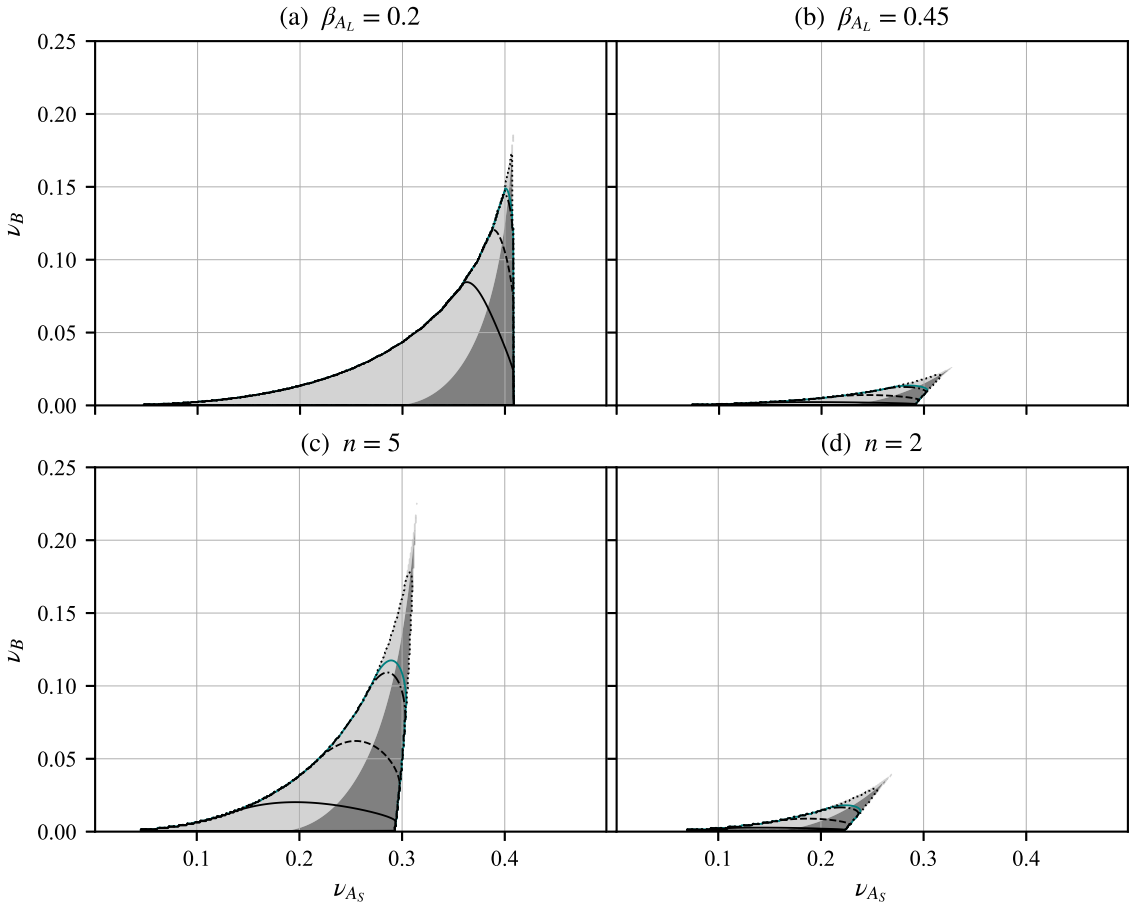

Figure 6. Top row: regions of single maxima (white) and two maxima (shaded) as a function of ν_{A_L} and ν_B with $\beta_{A_L} = 0.2$ and 0.45, for the two-component linear chain with random assembly. In the shaded regions, the darker (respectively, lighter) areas are where the maximum with the smaller (respectively, larger) wavenumber is higher. The solid contour line across the cusp indicates a wavenumber ratio $Q_r = 3.5$, with dashed, dash-dot, and dotted lines indicating wavenumber ratios of 2.5, 2.0, and 1.5, respectively. The teal line indicates where the wavenumber ratio is 1.93. Bottom row: we plot the results for the monodisperse versions with (c) $n = 5$ and (d) $n = 2$ in terms of equivalent values of ν_{A_L} and ν_B.

https://doi.org/10.1021/acs.macromol.3c00800
Macromolecules 2023, 56, 7847−7859

chain contributes $(P_{A_SB}G_BG_{A_S})^2P_{A_LB}G_B$, and so on. The infinite geometric series, with common factor $P_{A_SB}G_BG_{A_S}$, can readily be summed, for this and for the other interactions.[65] The outcome of these calculations is

$$
\begin{aligned}
S_{A_LA_L} &= N_{A_L}\Omega\rho\frac{\beta_{A_L}}{\beta_{A_L}+\nu_{A_S}\beta_{A_S}+\nu_B\beta_B}\left(j_{A_L}+h_{A_L}^2\frac{P_{A_LB}G_B}{1-P_{A_SB}G_{A_S}G_B}\right)\\
S_{A_LA_S} &= N_{A_L}\Omega\rho\frac{\nu_{A_S}\beta_{A_L}}{\beta_{A_L}+\nu_{A_S}\beta_{A_S}+\nu_B\beta_B}h_{A_L}h_{A_S}\frac{P_{A_SB}G_B}{1-P_{A_SB}G_{A_S}G_B}\\
S_{A_LB} &= N_{A_L}\Omega\rho\frac{\nu_B\beta_{A_L}}{\beta_{A_L}+\nu_{A_S}\beta_{A_S}+\nu_B\beta_B}h_{A_L}h_B\frac{1}{1-P_{A_SB}G_{A_S}G_B}\\
S_{A_SA_S} &= N_{A_L}\Omega\rho\frac{\nu_{A_S}^2\beta_{A_S}}{\beta_{A_L}+\nu_{A_S}\beta_{A_S}+\nu_B\beta_B}\left(j_{A_S}+2h_{A_S}^2\frac{P_{A_SB}G_B}{1-P_{A_SB}G_{A_S}G_B}\right)\\
S_{A_SB} &= N_{A_L}\Omega\rho\frac{\nu_{A_S}\nu_B\beta_{A_S}}{\beta_{A_L}+\nu_{A_S}\beta_{A_S}+\nu_B\beta_B}2h_{A_S}h_B\frac{1}{1-P_{A_SB}G_{A_S}G_B}\\
S_{BB} &= N_{A_L}\Omega\rho\frac{\nu_B^2\beta_B}{\beta_{A_L}+\nu_{A_S}\beta_{A_S}+\nu_B\beta_B}\left(j_B+2h_B^2\frac{P_{A_SB}G_{A_S}}{1-P_{A_SB}G_{A_S}G_B}\right)
\end{aligned}
\tag{21}
$$

The overall structure factors S_0^{AA}, S_0^{BB}, and S_0^{AB} are

$$
\begin{aligned}
S_0^{AA} &= S_{A_LA_L}+2S_{A_LA_S}+S_{A_SA_S}\\
S_0^{BB} &= S_{BB}\\
S_0^{AB} &= S_{A_LB}+S_{A_SB}
\end{aligned}
\tag{22}
$$

These are combined into the noninteracting structure factor expression in eq 4.

Thus, the noninteracting structure factor $S_0(q)$ is determined as a function of the normalized wavenumber and the three parameters: the block fraction β_{A_L} and the monomer fractions ν_{A_S} and ν_B. For fixed β_{A_L}, the regions of (ν_{A_S},ν_B) where there are two maxima in the structure factor are once again cusp-shaped (see Figure 6 for $\beta_{A_L}=0.2$ and $\beta_{A_L}=0.45$). The lines across the shaded part of the cusps indicate the ratio between the wavenumbers where the two peaks occur. When β_{A_L} is 0.2 (with $\beta_{A_S}=0.35$ and $\beta_B=0.45$), there are more A_S and B blocks than A_L blocks, so the polymer will form longer chains, and the region for two length scale phase separation is larger than with $\beta_{A_L}=0.45$ ($\beta_{A_S}=0.1625$ and $\beta_B=0.3875$). In both these cases, the length scale ratio corresponding to 12-fold symmetry is indicated by the teal line.

Direct mapping between the monodisperse fixed n and polydisperse random assembly versions of the two-component linear chain models is not possible because of the range of chain lengths possible in the second case, and because of the difference in architecture. But, roughly speaking, β_{A_L} is inversely proportional to the number of A_S and B blocks available in the polydisperse model, which is related to the number n of BA_S diblocks in the monodisperse case. However, for fixed n in the monodisperse case, it is possible to convert the parameters from (f_A,ϕ_A) in that case to (ν_{A_S},ν_B), but while keeping the n the same. The two length scale regions in the polydisperse case (Figure 6, top row, with $\beta_{A_L}=0.2$ and $\beta_{A_L}=0.45$) are comparable to the two length scale regions in the monodisperse case (Figure 6, bottom row, with $n=5$ and $n=2$). This supports the hypothesis that longer chains and the presence of A_S blocks encourage two length scale phase separation.

THREE-COMPONENT *ABC* STAR

For a polymer system with three components and with Fourier transformed monomer densities $\rho_{\mathbf{q}}^A$, $\rho_{\mathbf{q}}^B$, and $\rho_{\mathbf{q}}^C$ for A, B, and C monomer units, respectively, the procedure for calculating the free energy is similar to the two-component system, though imposing the incompressibility condition is more involved. The noninteracting (compressible) structure factor matrix M_q is a three-by-three matrix whose components are S_0^{AA}, ⋯, S_0^{CC}

$$
M_q=\begin{bmatrix}S_0^{AA} & S_0^{AB} & S_0^{AC}\\ S_0^{AB} & S_0^{BB} & S_0^{BC}\\ S_0^{AC} & S_0^{BC} & S_0^{CC}\end{bmatrix}=n_cN^2\begin{bmatrix}s_0^{AA} & s_0^{AB} & s_0^{AC}\\ s_0^{AB} & s_0^{BB} & s_0^{BC}\\ s_0^{AC} & s_0^{BC} & s_0^{CC}\end{bmatrix}
\tag{23}
$$

where, as discussed in the case of the two-component system, the S_0^{IJ} terms are proportional to $n_cN^2=\Omega\rho N$. With this scaling, the structure factor terms s_0^{IJ} depend only on the scaled wavenumber and on parameters that describe the architecture of the polymer.

We need the inverse of this matrix, which we write as

$$
M_q^{-1}=\frac{1}{\Omega\rho N}\begin{bmatrix}\Gamma^{AA} & \Gamma^{AB} & \Gamma^{AC}\\ \Gamma^{AB} & \Gamma^{BB} & \Gamma^{BC}\\ \Gamma^{AC} & \Gamma^{BC} & \Gamma^{CC}\end{bmatrix}
\tag{24}
$$

Then, the free energy functional is

$$
F(\{\rho_{\mathbf{q}}^A,\rho_{\mathbf{q}}^B,\rho_{\mathbf{q}}^C\})=\frac{1}{2}\sum_{\mathbf{q}}\begin{bmatrix}\rho_{\mathbf{q}}^A & \rho_{\mathbf{q}}^B & \rho_{\mathbf{q}}^C\end{bmatrix}\left(M_q^{-1}+\frac{1}{\Omega}\begin{bmatrix}V_{AA} & V_{AB} & V_{AC}\\ V_{AB} & V_{BB} & V_{BC}\\ V_{AC} & V_{BC} & V_{CC}\end{bmatrix}\right)\begin{bmatrix}\rho_{-\mathbf{q}}^A\\ \rho_{-\mathbf{q}}^B\\ \rho_{-\mathbf{q}}^C\end{bmatrix}
\tag{25}
$$

where the three-by-three matrix of V_{AA}, etc. expresses the interaction potential between the different monomer types, and will be written in terms of N times the Flory interaction parameters below.

The incompressibility in the system provides the constraint

$$
\rho_{\mathbf{q}}^C=-(\rho_{\mathbf{q}}^A+\rho_{\mathbf{q}}^B)
\tag{26}
$$

https://doi.org/10.1021/acs.macromol.3c00800
Macromolecules 2023, 56, 7847−7859

which can be used to reduce the three-by-three matrices in the free energy to two-by-two

$$F(\{\rho_{\mathbf{q}}^{A}, \rho_{\mathbf{q}}^{B}\}) = \frac{1}{2}\sum_{\mathbf{q}} [\rho_{\mathbf{q}}^{A} \quad \rho_{\mathbf{q}}^{B}] W_q \begin{bmatrix} \rho_{-\mathbf{q}}^{A} \\ \rho_{-\mathbf{q}}^{B} \end{bmatrix} \tag{27}$$

Here, W_q is a 2×2 matrix that contains all of the noninteracting structure factor terms and the interaction potentials between different types of monomers and is defined by

$$\Omega\rho N W_q = \begin{bmatrix} \Gamma^{AA} + \Gamma^{CC} - 2\Gamma^{AC} & \Gamma^{AB} - \Gamma^{BC} - \Gamma^{AC} + \Gamma^{CC} \\ \Gamma^{AB} - \Gamma^{BC} - \Gamma^{AC} + \Gamma^{CC} & \Gamma^{BB} + \Gamma^{CC} - 2\Gamma^{BC} \end{bmatrix} + N \begin{bmatrix} -2\chi_{AC} & \chi_{AB} - \chi_{BC} - \chi_{AC} \\ \chi_{AB} - \chi_{BC} - \chi_{AC} & -2\chi_{BC} \end{bmatrix} \tag{28}$$

Here, the Flory interaction parameters χ for the monomer pairs of A, B, and C blocks are defined by

$$\chi_{AB} = -\frac{\rho}{2}(V_{AA} + V_{BB} - 2V_{AB})$$
$$\chi_{BC} = -\frac{\rho}{2}(V_{BB} + V_{CC} - 2V_{BC})$$
$$\chi_{AC} = -\frac{\rho}{2}(V_{AA} + V_{CC} - 2V_{AC}) \tag{29}$$

where the χ_{AB}, χ_{BC}, and χ_{AC} describe the interaction between pairs of monomer types.

For the ABC star architecture, the S_0^{AA}, S_0^{AB}, $\cdots$ terms in the M_q matrix in eq 23 are computed using Read's method,[63] though only self-terms and coterms are needed as the polymer architecture is simpler than in the two-component system. For the ABC star block copolymer system with N monomer units, we write the length fractions of the A, B, and C arms as f_A, f_B, and f_C, respectively, with

$$f_A + f_B + f_C = 1 \tag{30}$$

The number of monomer units in each arm is then

$$\text{number of monomer units in the } A \text{ block}: N_A = f_A N$$
$$\text{number of monomer units in the } B \text{ block}: N_B = f_B N$$
$$\text{number of monomer units in the } C \text{ block}: N_C = f_C N \tag{31}$$

The noninteracting structure factor terms corresponding to the ABC star architecture are

$$S_0^{AA} = J_A = N_A^2 j_A$$
$$S_0^{BB} = J_B = N_B^2 j_B$$
$$S_0^{CC} = J_C = N_C^2 j_C$$
$$S_0^{AB} = H_A H_B = N_A N_B h_A h_B$$
$$S_0^{BC} = H_B H_C = N_B N_C h_B h_C$$
$$S_0^{AC} = H_A H_C = N_A N_C h_A h_C \tag{32}$$

Here, j_A, j_B, j_C, h_A, h_B, and h_C are the self-terms and coterms for the A, B, and C branches as in eq 7, respectively. These are functions of the normalized wavenumbers Q_A, Q_B, and Q_C

$$Q_A^2 = f_A Q^2$$
$$Q_B^2 = f_B Q^2$$
$$Q_C^2 = f_C Q^2 = (1 - f_A - f_B) Q^2 \tag{33}$$

where $Q^2 = \frac{b^2 N}{6} q^2$ as before. With this, now writing wavenumber dependence in terms of Q, and taking incompressibility into account, the matrix W_Q (and its eigenvalues) is proportional to $\frac{1}{\Omega\rho N} = \frac{1}{n_c N^2}$, and can otherwise be expressed as a function of the scaled wavenumber Q, the polymer block fractions f_A and f_B, and the interaction parameters $N\chi_{AB}$, $N\chi_{BC}$, and $N\chi_{AC}$.

With W_Q defined, the quadratic form in eq 27 is positive definite when the eigenvalues of W_Q are both positive, and phase separation occurs when the smallest eigenvalue of W_Q changes from positive to negative. The wavenumber(s) at which this occurs gives the length scale(s) at phase separation. We compute the eigenvalues of W_Q as functions of the scaled wavenumber Q: see Figure 7 for an example where the smaller eigenvalue of W_Q has two minima at zero, and so is on the verge of phase separation with two length scales in a ratio of 1.6.

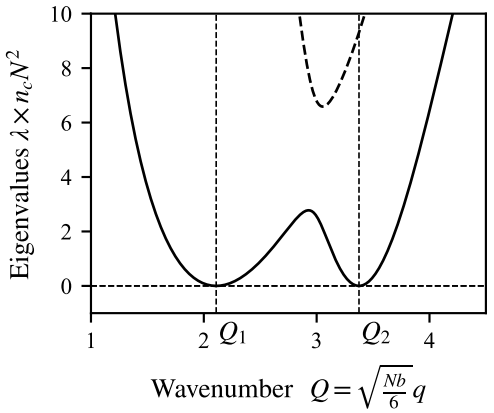

Figure 7. Two eigenvalues λ of W_Q as functions of the wavenumber Q. The two minima of the smaller eigenvalue (solid line) give the two length scales at phase separation. In this example, the wavenumbers are $Q_1 = 2.1096$ and $Q_2 = 3.3754$, with the ratio between the two wavenumbers being $Q_r = 1.60$. The other parameters are $f_A = 0.66775$, $f_B = f_C = 0.166125$, $N\chi_{AB} = N\chi_{AC} = 39.335$, and $N\chi_{BC} = 95.070$.

For the three-component model, the Q-dependent eigenvalues of W_Q depend on 5 parameters: f_A, f_B, $N\chi_{AB}$, $N\chi_{BC}$, and $N\chi_{AC}$, with $f_C = 1 - (f_A + f_B)$. Hence, achieving instability to phase separation simultaneously at two length scales depends both on the ratios of the interaction parameters and on the molecular composition (this is in contrast to the two-component case, where polymer composition alone determines the length scales of instability). We explore this parameter space at several fixed values of the ratio of χ_{AC} to χ_{AB}, defining $\frac{\chi_{AC}}{\chi_{AB}} = \xi$. The first step is to select a desired ratio of wavenumbers Q_r (for example, $Q_r = 1.6$) and a value of ξ (for example, $\xi = 1$), taking $f_B = f_C$ as a starting point. If $\lambda(Q)$ is the smaller of the two eigenvalues, and the two minima of $\lambda(Q)$ are at wavenumbers Q_1 and $Q_2 = Q_r Q_1$, the four equations for a zero double minimum of $\lambda(Q)$, as illustrated in Figure 7, are

https://doi.org/10.1021/acs.macromol.3c00800
Macromolecules 2023, 56, 7847−7859

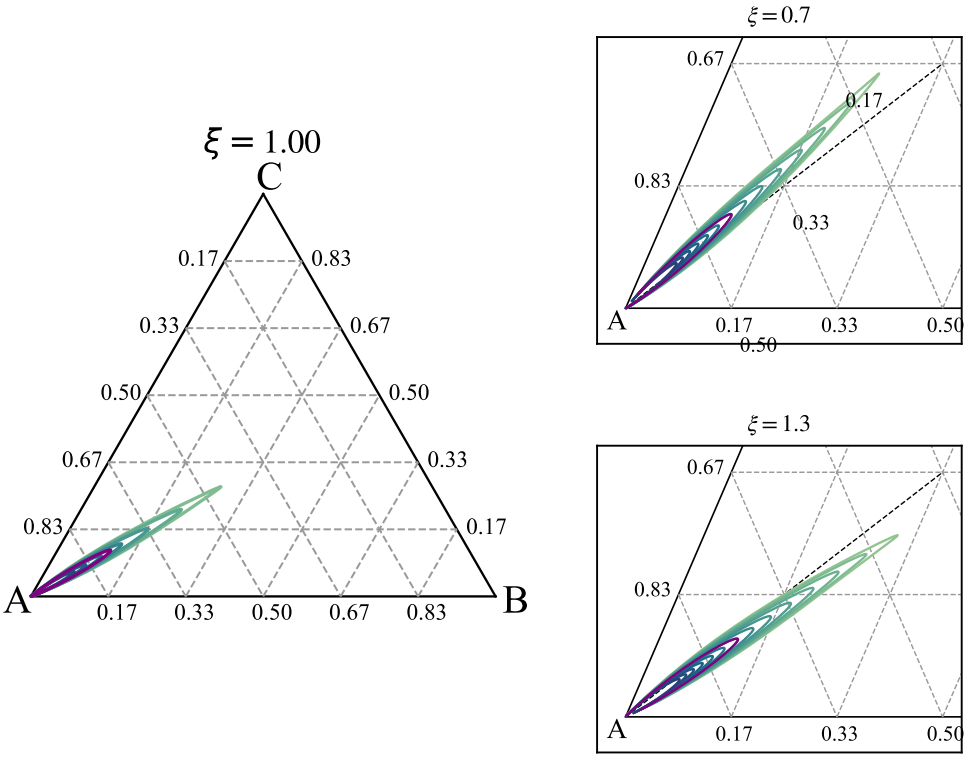

Figure 8. Curves of constant wavenumber ratio Q_r, shown as contour plots in (f_A, f_B, f_C) diagrams, for three choices of ξ: $\xi = 1$, 0.7, and 1.3. The outer contour in the petal-shaped regions is $Q_r = 1.2$, with Q_r increasing to 2.4 in steps of 0.2 in the $\xi = 1$ case and to 2.5 in steps of 0.1 in the other two cases. The purple contour is $Q_r = 1.93$.

$$\lambda(Q_1) = 0; \quad \lambda(Q_2) = 0$$
$$\left.\frac{d\lambda}{dQ}\right|_{Q_1} = 0; \quad \left.\frac{d\lambda}{dQ}\right|_{Q_2} = 0 \tag{34}$$

We solve these four equations for Q_1 and the values of the parameters f_A, χ_{AB}, and χ_{BC}, with $\chi_{AC} = \xi\chi_{AB}$ and $f_B = f_C = \frac{1}{2}(1 - f_A)$. This allows us to identify, for the choice of Q_r, for the choice that $f_B = f_C$ and for the chosen ratio between χ_{AB} and χ_{AC}, the other parameters at which phase separation occurs. We then keep the choice of Q_r and the ratio between χ_{AB} and χ_{AC} fixed, but allow $f_B \neq f_C$ to compute nearby solutions to the same four equations. In this way, we build up curves in the (f_A, f_B, f_C) space on which phase separation occurs at two length scales simultaneously. We choose other values of Q_r to get several curves in that space, as illustrated in Figure 8, for three choices of ξ.

In Figure 8, we focus on the case where the A block has longer arms, so we take $f_A \geq \frac{1}{3}$. There will be other curves of two length scale phase separation in the other corners of the triangle. The outer contour in the petal-shaped regions of two length scale phase separation is $Q_r = 1.2$, with Q_r increasing on the inner contours, with the larger Q_r corresponding to f_A closer to 1. In the case $\xi = 1$, when B and C have the same interaction potential with A, the petal region is symmetric under reflections in the $f_B = f_C$ diagonal (dotted line). With smaller ξ ($\chi_{AC} < \chi_{AB}$) the petal bends upward toward the C region with larger f_C. Similarly, with larger ξ, the petal region bends downward toward the B region. The region of having two length scales is quite narrow and is located in the parameter region where A is long and the other two are of similar sizes. Although we have only computed the contours up to $Q_r = 2.5$, we expect that larger length scale ratios would be possible for f_A closer to 1.

CONCLUSIONS

We have investigated the length scales that emerge at the point of phase separation in two classes of block copolymer models. The first has alternating lengths of polymers of two different types, and the second has three different monomer types in a terpolymer star configuration. In both cases, we find that as well as having a single length scale at phase separation, it is possible to design the polymers so that two length scales emerge. The transition from one to two length scales occurs at a point (a cusp) in the parameter space when the length scale ratio is one. Beyond this cusp, the length scale ratio can be made much larger than one. In principle, the ideas and techniques developed here apply to arbitrary configurations of different types of monomers: we have explored only the simplest examples.

We have identified experimentally accessible architectures that have phase separation at the length scale ratio 1.93 that favors 12-fold quasicrystals. In the $A_L(BA_S)_n$ case, the smallest molecule has $n = 1.5$, and the parameters are $(f_A, \phi_A) \approx (0.7, 0.9)$ (Figure 4a), which corresponds to an $A_L BA_S B$ structure, with A_L being 70% of the length of the chain, the two B's are about 2.7% each and the A_S is 24.6%. For molecules with more repeating BA_S units, the parameters that have phase separation with two length scales have larger proportions of B and smaller proportions of A_L, but these will be harder to manufacture. In the case of random assembly, an example choice of parameters is a mixture that is 20% A_L, 35% A_S, and 45% B, where the lengths of the three chains are in a ratio A_L:A_S:B = 1:0.39:0.14 (see Figure 6a). Of course, attention will also need to be paid to the values of $N\chi$ that are needed at the point of instability, and the relative heights of the peaks in the structure factor. Prior work in

https://doi.org/10.1021/acs.macromol.3c00800
Macromolecules 2023, 56, 7847−7859

this area[56] took $\phi_A = \phi_B$; our work covers parameter values that would allow considerably easier synthesis of the polymers, in regimes that ought to favor the formation of quasicrystals.

Up until now, experimental observations in linear block copolymer melts have mainly found only relatively simple structures, such as hexagons and lamellae, or hierarchical two length scale structures, such as lamellae-within-lamellae with several layer thicknesses.[66,67] There are indications that more complex structures can be stable: self-consistent field theory studies of linear *ABAB* tetrablock copolymers[68] report structures including a lamella−sphere phase and a gyroid phase. Cylindrical 12-fold quasicrystal approximants in linear *ABCB* terpolymer melts have also been found in self-consistent field theory calculations,[69] and the Fourier transform images reported in that paper have two length scales in the characteristic 1.93 ratio.

To our knowledge, ours is the first presentation of phase separation with two length scales in the *ABC* star terpolymer system. This is a system where quasicrystals and close approximants have been found experimentally.[5] As in the $A_L(BA_S)_n$ case above, values of the three $N\chi$ parameters are quite large, suggesting that self-consistent field theory or strong segregation theory would be an appropriate next step.

Of course, our RPA calculations are only the first step: these reveal the length scales but not the final stable structures. Subsequent steps, involving weak segregation theory,[70] self-consistent field theory,[53,54,68,69,71] strong segregation theory,[72] etc., have been carried out by several authors, but finding quasicrystals has been challenging, partly because the calculations in all of these cases are quite demanding. The final structure will be influenced by the length scale ratio and the heights of the peaks in the structure factor or values of the eigenvalues in the dispersion relation. The examples in Figures 3 and 7 are where these are equal at the two length scales, but the shaded regions in Figures 4 and 6 indicate where one or other peak height is larger. In some (phase field crystal) models of soft matter quasicrystals, fully developed quasicrystals are found where the peaks have the same or similar heights,[29,31] while in other (density functional theory) models, quasicrystals are found where the peaks have quite different heights.[36,37] In the models, the stability of fully developed quasicrystals depends not only on the eigenvalues at the two length scales but also on the (negative) eigenvalues at other length scales that might feature in regular crystalline orderings that compete with quasicrystals.[38] Our work provides this information and so should provide useful starting parameter values with two length scale phase separation, which should be a good place to start a search for quasicrystals or their approximants, experimentally or using more sophisticated theoretical methods.

AUTHOR INFORMATION

Corresponding Authors

Merin Joseph − *School of Mathematics, University of Leeds, Leeds LS2 9JT, U.K.;* orcid.org/0000-0002-0441-9365; Email: fsmj@leeds.ac.uk

Daniel J. Read − *School of Mathematics, University of Leeds, Leeds LS2 9JT, U.K.;* orcid.org/0000-0003-1194-9273; Email: D.J.Read@leeds.ac.uk

Alastair M. Rucklidge − *School of Mathematics, University of Leeds, Leeds LS2 9JT, U.K.;* orcid.org/0000-0003-2985-0976; Email: A.M.Rucklidge@leeds.ac.uk

Complete contact information is available at: https://pubs.acs.org/10.1021/acs.macromol.3c00800

Notes

The authors declare no competing financial interest.

ACKNOWLEDGMENTS

The authors thank Profs Andrew Archer, Ron Lifshitz, An-Chang Shi, and Bart Vorselaars for stimulating conversations, and Joanna Tumelty for advice on numerical methods. MJ is grateful for a PhD studentship from the Soft Matter and Functional Interfaces (SOFI) Centre for Doctoral Training (EP/L015536/1) and the School of Mathematics, University of Leeds. AMR is grateful for support from the Engineering and Physical Sciences Research Council (EP/P015611/1) and the Leverhulme Trust (RF-2018-449/9). The data associated with this paper are openly available from the University of Leeds Data Repository (10.5518/1333).[73] For the purpose of open access, the authors have applied a Creative Commons Attribution (CC BY) license to any Author Accepted Manuscript version arising from this submission.

REFERENCES

(1) Lifshitz, R.; Diamant, H. Soft quasicrystals - Why are they stable? *Philos. Mag.* **2007**, *87*, 3021−3030.

(2) Shechtman, D.; Blech, I.; Gratias, D.; Cahn, J. W. Metallic phase with long-range orientational order and no translational symmetry. *Phys. Rev. Lett.* **1984**, *53*, 1951−1953.

(3) Zeng, X. B.; Ungar, G.; Liu, Y. S.; Percec, V.; Dulcey, S. E.; Hobbs, J. K. Supramolecular dendritic liquid quasicrystals. *Nature* **2004**, *428*, 157−160.

(4) Jayaraman, A.; Baez-Cotto, C. M.; Mann, T. J.; Mahanthappa, M. K. Dodecagonal quasicrystals of oil-swollen ionic surfactant micelles. *Proc. Natl. Acad. Sci. U.S.A.* **2021**, *118*, No. e2101598118.

(5) Hayashida, K.; Dotera, T.; Takano, A.; Matsushita, Y. Polymeric Quasicrystal: Mesoscopic Quasicrystalline Tiling in *ABC* Star Polymers. *Phys. Rev. Lett.* **2007**, *98*, No. 195502.

(6) Bates, F. S.; Fredrickson, G. H. Block Copolymers-Designer Soft Materials. *Phys. Today* **1999**, *52*, 32−38.

(7) Gillard, T. M.; Lee, S.; Bates, F. S. Dodecagonal quasicrystalline order in a diblock copolymer melt. *Proc. Natl. Acad. Sci. U.S.A.* **2016**, *113*, 5167−5172.

(8) Schulze, M. W.; Lewis, R. M., III; Lettow, J. H.; Hickey, R. J.; Gillard, T. M.; Hillmyer, M. A.; Bates, F. S. Conformational asymmetry and quasicrystal approximants in linear diblock copolymers. *Phys. Rev. Lett.* **2017**, *118*, No. 207801.

(9) Yue, K.; Huang, M.; Marson, R. L.; He, J.; Huang, J.; Zhou, Z.; Wang, J.; Liu, C.; Yan, X.; Wu, K.; Guo, Z.; Liu, H.; Zhang, W.; Ni, P.; Wesdemiotis, C.; Zhang, W. B.; Glotzer, S. C.; Cheng, S. Z. D. Geometry induced sequence of nanoscale Frank-Kasper and quasicrystal mesophases in giant surfactants. *Proc. Natl. Acad. Sci. U.S.A.* **2016**, *113*, 14195−14200.

(10) Zeng, X.; Glettner, B.; Baumeister, U.; Chen, B.; Ungar, G.; Liu, F.; Tschierske, C. A columnar liquid quasicrystal with a honeycomb structure that consists of triangular, square and trapezoidal cells. *Nat. Chem.* **2023**, *15*, 625−632.

(11) Chang, A. B.; Bates, F. S. The ABCs of Block Polymers. *Macromolecules* **2020**, *53*, 2765−2768.

(12) Huang, M.; Yue, K.; Wang, J.; Hsu, C.-H.; Wang, L.; Cheng, S. Z. D. Frank-Kasper and related quasicrystal spherical phases in macromolecules. *Sci. China Chem.* **2018**, *61*, 33−45.

(13) Vitiello, M. S.; Nobile, M.; Ronzani, A.; Tredicucci, A.; Castellano, F.; Talora, V.; Li, L.; Linfield, E. H.; Davies, A. G. Photonic quasi-crystal terahertz lasers. *Nat. Commun.* **2014**, *5*, No. 5884.

(14) Sinelnik, A. D.; Shishkin, I. I.; Yu, X.; Samusev, K. B.; Belov, P. A.; Limonov, M. F.; Ginzburg, P.; Rybin, M. V. Experimental Observation of Intrinsic Light Localization in Photonic Icosahedral Quasicrystals. *Adv. Opt. Mater.* **2020**, *8*, No. 2001170.

(15) Edwards, W. S.; Fauve, S. Patterns and Quasi-patterns in the Faraday Experiment. *J. Fluid Mech.* **1994**, *278*, 123−148.
(16) Kudrolli, A.; Pier, B.; Gollub, J. P. Superlattice patterns in surface waves. *Phys. D* **1998**, *123*, 99−111.
(17) Arbell, H.; Fineberg, J. Pattern formation in two-frequency forced parametric waves. *Phys. Rev. E* **2002**, *65*, No. 036224.
(18) Pampaloni, E.; Ramazza, P. L.; Residori, S.; Arecchi, F. T. Two-Dimensional Crystals and Quasicrystals in Nonlinear Optics. *Phys. Rev. Lett.* **1995**, *74*, 258−261.
(19) Smart, T.; Lomas, H.; Massignani, M.; Flores-Merino, M. V.; Perez, L. R.; Battaglia, G. Block copolymer nanostructures. *Nano Today* **2008**, *3*, 38−46.
(20) Chernyy, S.; Kirkensgaard, J. J. K.; Mahalik, J. P.; Kim, H.; Arras, M. M.; Kumar, R.; Sumpter, B. G.; Smith, G. S.; Mortensen, K.; Russell, T. P.; Almdal, K. Bulk and surface morphologies of ABC miktoarm star terpolymers composed of PDMS, PI, and PMMA arms. *Macromolecules* **2018**, *51*, 1041−1051.
(21) Zhang, W. B.; Viñals, J. Square patterns and quasipatterns in weakly damped Faraday waves. *Phys. Rev. E* **1996**, *53*, R4283−R4286.
(22) Lifshitz, R.; Petrich, D. M. Theoretical model for Faraday waves with multiple-frequency forcing. *Phys. Rev. Lett.* **1997**, *79*, 1261−1264.
(23) Porter, J.; Topaz, C. M.; Silber, M. Pattern control via multifrequency parametric forcing. *Phys. Rev. Lett.* **2004**, *93*, No. 034502.
(24) Rucklidge, A. M.; Silber, M.; Skeldon, A. C. Three-Wave Interactions and Spatiotemporal Chaos. *Phys. Rev. Lett.* **2012**, *108*, No. 074504.
(25) Skeldon, A. C.; Rucklidge, A. M. Can weakly nonlinear theory explain Faraday wave patterns near onset? *J. Fluid Mech.* **2015**, *777*, 604−632.
(26) Castelino, J. K.; Ratliff, D. J.; Rucklidge, A. M.; Subramanian, P.; Topaz, C. M. Spatiotemporal chaos and quasipatterns in coupled reaction-diffusion systems. *Phys. D* **2020**, *409*, No. 132475.
(27) Achim, C. V.; Schmiedeberg, M.; Löwen, H. Growth Modes of Quasicrystals. *Phys. Rev. Lett.* **2014**, *112*, No. 255501.
(28) Jiang, K.; Tong, J.; Zhang, P.; Shi, A.-C. Stability of two-dimensional soft quasicrystals in systems with two length scales. *Phys. Rev. E* **2015**, *92*, No. 042159.
(29) Subramanian, P.; Archer, A. J.; Knobloch, E.; Rucklidge, A. M. Three-Dimensional Icosahedral Phase Field Quasicrystal. *Phys. Rev. Lett.* **2016**, *117*, No. 075501.
(30) Jiang, K.; Zhang, P.; Shi, A.-C. Stability of icosahedral quasicrystals in a simple model with two-length scales. *J. Phys.: Condens. Matter* **2017**, *29*, No. 124003.
(31) Savitz, S.; Babadi, M.; Lifshitz, R. Multiple-scale structures: from Faraday waves to soft-matter quasicrystals. *IUCrJ* **2018**, *5*, 247−268.
(32) Jiang, Z.; Quan, S.; Xu, N.; He, L.; Ni, Y. Growth modes of quasicrystals involving intermediate phases and a multistep behavior studied by phase field crystal model. *Phys. Rev. Mater.* **2020**, *4*, No. 023403.
(33) Tang, S.; Wang, Z.; Wang, J.; Jiang, K.; Liang, C.; Ma, Y.; Liu, W.; Du, Y. An atomic scale study of two-dimensional quasicrystal nucleation controlled by multiple length scale interactions. *Soft Matter* **2020**, *16*, 5718−5726.
(34) Liang, C.; Jiang, K.; Tang, S.; Wang, J.; Ma, Y.; Liu, W.; Du, Y. Molecular-Level Insights into the Nucleation Mechanism of One-Component Soft Matter Icosahedral Quasicrystal Studied by Phase-Field Crystal Simulations. *Cryst. Growth Des.* **2022**, *22*, 2637−2643.
(35) Barkan, K.; Diamant, H.; Lifshitz, R. Stability of quasicrystals composed of soft isotropic particles. *Phys. Rev. B* **2011**, *83*, No. 172201.
(36) Archer, A. J.; Rucklidge, A. M.; Knobloch, E. Quasicrystalline order and a crystal-liquid state in a soft-core fluid. *Phys. Rev. Lett.* **2013**, *111*, No. 165501.
(37) Archer, A. J.; Rucklidge, A. M.; Knobloch, E. Soft-core particles freezing to form a quasicrystal and a crystal-liquid phase. *Phys. Rev. E* **2015**, *92*, No. 012324.
(38) Ratliff, D. J.; Archer, A. J.; Subramanian, P.; Rucklidge, A. M. Which wave numbers determine the thermodynamic stability of soft matter quasicrystals? *Phys. Rev. Lett.* **2019**, *123*, No. 148004.
(39) Subramanian, P.; Archer, A. J.; Knobloch, E.; Rucklidge, A. M. Snaking without subcriticality: grain boundaries as non-topological defects. *IMA J. Appl. Math.* **2021**, *86*, 1164−1180.
(40) Scacchi, A.; Somerville, W. R. C.; Buzza, D. M. A.; Archer, A. J. Quasicrystal formation in binary soft matter mixtures. *Phys. Rev. Res.* **2020**, *2*, No. 032043(R).
(41) Walters, M. C.; Subramanian, P.; Archer, A. J.; Evans, R. Structural crossover in a model fluid exhibiting two length scales: repercussions for quasicrystal formation. *Phys. Rev. E* **2018**, *98*, No. 012606.
(42) Engel, M.; Trebin, H. R. Self-assembly of monatomic complex crystals and quasicrystals with a double-well interaction potential. *Phys. Rev. Lett.* **2007**, *98*, No. 225505.
(43) Barkan, K.; Engel, M.; Lifshitz, R. Controlled Self-Assembly of Periodic and Aperiodic Cluster Crystals. *Phys. Rev. Lett.* **2014**, *113*, No. 098304.
(44) Damasceno, P. F.; Engel, M.; Glotzer, S. C. Predictive Self-Assembly of Polyhedra into Complex Structures. *Science* **2012**, *337*, 453−457.
(45) Je, K.; Lee, S.; Teich, E. G.; Engel, M.; Glotzer, S. C. Entropic formation of a thermodynamically stable colloidal quasicrystal with negligible phason strain. *Proc. Natl. Acad. Sci. U.S.A.* **2021**, *118*, 118.
(46) Dotera, T.; Oshiro, T.; Ziherk, P. Mosaic two-lengthscale quasicrystals. *Nature* **2014**, *506*, 208−211.
(47) Dotera, T.; Bekku, S.; Ziherl, P. Bronze-mean hexagonal quasicrystal. *Nat. Mater.* **2017**, *16*, 987−992.
(48) Silber, M.; Topaz, C. M.; Skeldon, A. C. Two-frequency forced Faraday waves: weakly damped modes and pattern selection. *Phys. D* **2000**, *143*, 205−225.
(49) Rucklidge, A. M.; Silber, M. Design of Parametrically Forced Patterns and Quasipatterns. *SIAM J. Appl. Dyn. Syst.* **2009**, *8*, 298−347.
(50) Bak, P. Phenomenological Theory of Icosahedral Incommensurate ("Quasiperiodic") Order in Mn-Al Alloys. *Phys. Rev. Lett.* **1985**, *54*, 1517−1519.
(51) Archer, A. J.; Dotera, T.; Rucklidge, A. M. Rectangle-triangle soft-matter quasicrystals with hexagonal symmetry. *Phys. Rev. E* **2022**, *106*, No. 044602.
(52) Christiansen, B.; Alstrom, P.; Levinsen, M. T. Dissipation and ordering in capillary waves at high aspect ratios. *J. Fluid Mech.* **1995**, *291*, 323−341.
(53) Li, W.; Xu, Y.; Zhang, G.; Qiu, F.; Yang, Y.; Shi, A.-C. Real-space self-consistent mean-field theory study of ABC star triblock copolymers. *J. Chem. Phys.* **2010**, *133*, No. 064904.
(54) Xu, W.; Jiang, K.; Zhang, P.; Shi, A.-C. A Strategy to Explore Stable and Metastable Ordered Phases of Block Copolymers. *J. Phys. Chem. B* **2013**, *117*, 5296−5305.
(55) Tyler, C. A.; Qin, J.; Bates, F. S.; Morse, D. C. SCFT Study of Nonfrustrated ABC Triblock Copolymer Melts. *Macromolecules* **2007**, *40*, 4654−4668.
(56) Nap, R.; Kok, C.; Ten Brinke, G.; Kuchanov, S. Microphase separation at two length scales. *Eur. Phys. J. E* **2001**, *4*, 515−519.
(57) Nap, R.; Sushko, N.; Erukhimovich, I.; Ten Brinke, G. Double Periodic Lamellar-in-Lamellar Structure in Multiblock Copolymer Melts with Competing Length Scales. *Macromolecules* **2006**, *39*, 6765−6770.
(58) Kuchanov, S.; Pichugin, V.; Ten Brinke, G. Phase transitions in block copolymers resulting in a discontinuous change of the spatial period of mesophases. *Europhys. Lett. (EPL)* **2006**, *76*, 959−964.
(59) Kim, J. K.; Kimishima, K.; Hashimoto, T. Random-phase approximation calculation of the scattering function for multi-component polymer systems. *Macromolecules* **1993**, *26*, 125−136.
(60) de Gennes, P. G. Theory of X-ray scattering by liquid macromolecules with heavy atom labels. *J. Phys.* **1970**, *31*, 235−238.
(61) Leibler, L. Theory of microphase separation in block copolymers. *Macromolecules* **1980**, *13*, 1602−1617.
(62) Rubinstein, M.; Colby, R. H. *Polymer Physics*; Oxford University Press: New York, 2003.
(63) Read, D. J. Mean field theory for phase separation during polycondensation reactions and calculation of structure factors for

https://doi.org/10.1021/acs.macromol.3c00800
Macromolecules 2023, 56, 7847−7859

copolymers of arbitrary architecture. *Macromolecules* **1998**, *31*, 899−911.
(64) Bentley, D. C.; Rucklidge, A. M. Localized patterns in a generalized Swift-Hohenberg equation with a quartic marginal stability curve. *IMA J. Appl. Math.* **2021**, *86*, 944−983.
(65) Joseph, M. Searching for quasicrystals in block copolymer phase separation. Ph.D. thesis University of Leeds, 2023.
(66) Faber, M.; Voet, V. S. D.; ten Brinke, G.; Loos, K. Preparation and self-assembly of two-length-scale $A-b-(B-b-A)_n-b-B$ multiblock copolymers. *Soft Matter* **2012**, *8*, 4479−4485.
(67) Ritzenthaler, S.; Court, F.; Girard-Reydet, E.; Leibler, L.; Pascault, J. P. ABC Triblock Copolymers/Epoxy-Diamine Blends. 2. Parameters Controlling the Morphologies and Properties. *Macromolecules* **2003**, *36*, 118−126.
(68) Zhao, B.; Jiang, W.; Chen, L.; Li, W.; Qiu, F.; Shi, A.-C. Emergence and Stability of a Hybrid Lamella-Sphere Structure from Linear ABAB Tetrablock Copolymers. *ACS Macro Lett.* **2018**, *7*, 95−99.
(69) Duan, C.; Zhao, M.; Qiang, Y.; Chen, L.; Li, W.; Qiu, F.; Shi, A.-C. Stability of Two-Dimensional Dodecagonal Quasicrystalline Phase of Block Copolymers. *Macromolecules* **2018**, *51*, 7713−7721.
(70) Erukhimovich, I. Y. Weak segregation theory and non-conventional morphologies in the ternary ABC triblock copolymers. *Eur. Phys. J. E* **2005**, *18*, 383−406.
(71) Jiang, K.; Zhang, J.; Liang, Q. Self-assembly of asymmetrically interacting ABC star triblock copolymer melts. *J. Phys. Chem. B* **2015**, *119*, 14551−14562.
(72) Gemma, T.; Hatano, A.; Dotera, T. Monte Carlo simulations of the morphology of ABC star polymers using the diagonal bond method. *Macromolecules* **2002**, *35*, 3225−3237.
(73) Joseph, M.; Read, D. J.; Rucklidge, A. M. *Dataset for "Design of Linear Block Copolymers and ABC Star Terpolymers that Produce Two Length Scales at Phase Separation"*, University of Leeds Data Repository, 2023, DOI: 10.5518/1333.

https://doi.org/10.1021/acs.macromol.3c00800
Macromolecules 2023, 56, 7847−7859